This article has been accepted for publication in a future issue of this journal, but has not been fully edited. Content may change prior to final publication. Citation information: DOI 10.1109/LPT.2018.2826999, IEEE Photonics Technology Letters

$Al_{0.8}In_{0.2}As_{0.23}Sb_{0.77}$ Avalanche Photodiodes

Ann-Katheryn Rockwell*, Yuan Yuan*, Andrew H. Jones, Stephen D. March, Seth R. Bank, and Joe C. Campbell

Abstract — We report avalanche photodiodes (APDs) fabricated from the digital alloy $Al_{0.8}In_{0.2}As_{0.23}Sb_{0.77}$ (lattice-matched to GaSb). The APDs exhibit high avalanche multiplication, and low excess noise.

***Index Terms* — Avalanche photodiodes, photodetectors, optoelectronic devices**

I. Introduction

Avalanche photodiodes have been widely used in telecommunication, military, and research applications. Relative to p-i-n photodiodes, APDs can provide higher receiver sensitivity owing to their internal gain [1], [2]. However, the gain, which originates from impact ionization, is also the source of noise for which the figure of merit is the excess noise factor $F<M>$. In the local field model [3], the excess noise factor can be expressed as: $F < M >= kM + (1 - k)(2 - 1/M)$, where k is ratio of the hole ionization coefficient, β to the electron ionization coefficient, α, and M is multiplication gain. While the excess noise factor increases with gain, it increases more slowly for low values of k. Thus, k becomes a secondary figure of merit to describe the noise of the APD. Therefore, it is advantageous to utilize materials with low values of k. Another important figure of merit is the gain-bandwidth product. Emmons has shown that smaller k also enables higher gain-bandwidth products [4]. Recently, Shiyu Xie *et al*. have reported that AlGaAsSb APDs, whose k value is ~ 0.1, exhibit a high gain-bandwidth product of 424 GHz [5], [6].

In this work, we demonstrate an $Al_{0.8}In_{0.2}As_{0.23}Sb_{0.77}$ p-i-n structure APD that achieves k value < 0.07, multiplication gain > 480, and low dark current.

II. Device Structure and Fabrication

Previously, we have demonstrated the high quality growth of $Al_xIn_{1-x}As_ySb_{1-y}$ digital alloys lattice matched to GaSb for use in staircase, SACM and p-i-n APDs with x = 0.3-0.7. In this work, we extend our study of p-i-n APDs to include x = 0.8. The $Al_{0.8}In_{0.2}As_{0.23}Sb_{0.77}$ (written as $Al_{0.8}$InAsSb in the following) epitaxial layers were grown on n-type Te-doped GaSb (001) substrates by solid-source molecular beam epitaxy. The 10 monolayer (ML) or 3.05 nm, period digital alloys were grown comprising four binary alloys AlSb, AlAs, InSb, and InAs. The resulting shutter sequence was AlSb, AlAs, AlSb, InSb, InAs, Sb [7], [8], [9].

A cross-sectional schematic of the $Al_{0.8}$InAsSb p-i-n structure APD is shown in Fig. 1. From the top to bottom, the structure consists a 100 nm GaSb p-type top contact layer, a 100 nm $Al_{0.8}$InAsSb p-type layer, a 1000 nm $Al_{0.8}$InAsSb unintentionally-doped multiplication layer, a 100 nm $Al_{0.8}$InAsSb n-type layer, a 100 nm GaSb n-type bottom contact layer, and an n-type GaSb substrate. The top three layers are p-type doped using Be, and the other layers are n-type doped with Te.

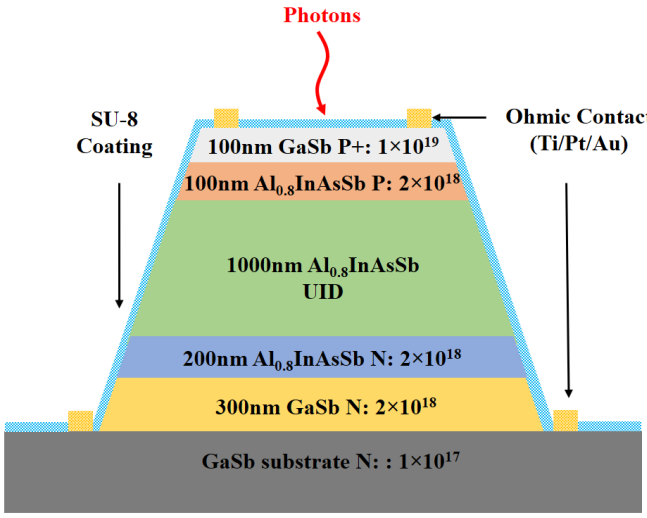

Figure 1. Schematic cross section of $Al_{0.8}$InAsSb p-i-n APD.

The mesas were defined by standard photolithography and formed by wet etching in a 5:1:5 solution of $HCl:H_2O_2:H_2O$. Ti/Pt/Au was deposited as the top and bottom contacts by electron-beam evaporation [10], [11]. After lift-off of the metals, SU-8 was spun on the sidewall as a surface passivation.

III. Results and Discussion

In this paper, all measurements were carried out at room temperature. Figure 2 shows the photocurrent, dark current, and gain versus bias voltage of a 100 μm-diameter $Al_{0.8}$InAsSb p-i-

This work was supported by Army Research Office and DARPA under contract W911NF-10-1-0391.
* These authors contributed equally to this work.
Y. Yuan, A. Jones, and J. C. Campbell are with the Electrical and Computer Engineering Department, University of Virginia, Charlottesville, VA 22904, USA (e-mail: jccuva@virginia.edu).
A.-K. Rockwell, S. D. March, and S. R. Bank are with Electrical and Computer Engineering Department, University of Texas at Austin, 1616 Guadalupe St. Austin, TX 7875 (email: sbank@utexas.edu)
Color versions of one or more of the figures in this letter are available online at http://ieeexplore.ieee.org.

This article has been accepted for publication in a future issue of this journal, but has not been fully edited. Content may change prior to final publication. Citation information: DOI 10.1109/LPT.2018.2826999, IEEE Photonics Technology Letters

n APD. The APD was illuminated with 10 μW 850 nm laser, and the gain curve is plotted by choosing the unity gain point at -24.5 V. High gain of 489 was achieved at -32.5 V bias. There are three slopes in the photocurrent: the first gradual slope (from 0 to 11 V) might be caused by the heterojunction barrier [12], the second slope (from 11 to 24.5 V) is because of changes in carrier collection efficiency, and after 24.5 V the multiplication gain makes the third slope of the photocurrent steeper.

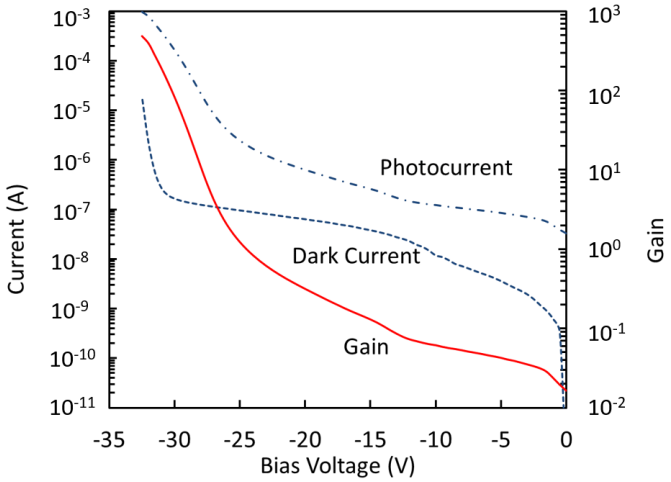

Figure 2. Photocurrent (solid line), dark current (dash dot line), and gain (dash line) versus bias voltage for a 80 μm-diameter $Al_{0.8}InAsSb$ p-i-n APD.

Since the photocurrent increases continuously with bias and does not exhibit a flat, voltage-independent region, the unity gain point is not obvious. The reason for this is voltage-dependent responsivity at lower bias. Owing to high background doping (~ 10^{17} cm^{-3}) in the 1000 nm-thick $Al_{0.8}InAsSb$ p^- multiplication layer, the carrier collection efficiency improves with increasing bias as the depletion moves closer to the surface. This was confirmed by capacitance-voltage measurements, which were used to calculate the depletion width. Figure 3 shows the capacitance and depletion width versus voltage, where is assumed the dielectric constant of $Al_{0.8}InAsSb$ is about 14. And since the device is wet etched, its effective diameter is a little bit smaller than 100 μm, here use 98 μm to calculate capacitance.

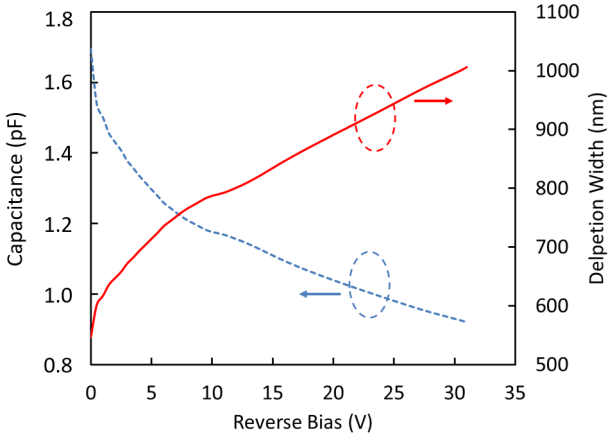

Figure 3. Capacitance and depletion width versus reverse bias of a 100 μm-diameter $Al_{0.8}InAsSb$ p-i-n APD.

In order to determine the gain curve in Fig. 2, we have developed a model to fit the external quantum efficiency in order to find the unity gain point. Since the background doping in the multiplication layer is p-type, the edge of the depletion layer will move toward the surface with increasing reverse bias, which, in turn, will result in increased responsivity as more carriers are collected. This is illustrated in Fig. 4.

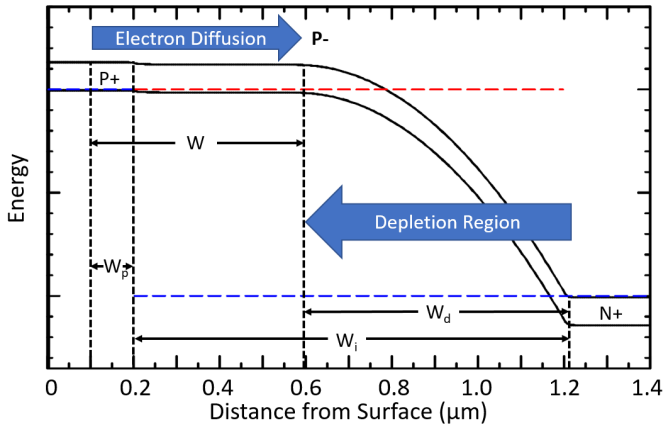

Figure 4. Illustration of mechanism for voltage-dependent responsivity.

The total current density of the device consists the drift current density that is generated in the depletion layer and the diffusion current density that is generated outside the depletion layer and collected by diffusion [13]. The current density can be expressed as:

$$J_{tot} = J_{dr} + J_{diff}, \quad (1)$$

$$J_{dr} = q\emptyset_0[exp(-\alpha W) - \exp(-\alpha W_p - \alpha W_i)], \quad (2)$$

$$J_{diff} = q[\frac{\emptyset_0 \alpha L_n}{1-\alpha^2 L_n^2} exp\left(-\frac{W}{L_n}\right) - \frac{\emptyset_0 \alpha^2 L_n^2}{1-\alpha^2 L_n^2} exp(-\alpha W)], \quad (3)$$

where the $\emptyset_0$ is the incident photon flux per unit area, α is absorption coefficient and L_n is the electron diffusion length, The distance from the surface to the edge of the depletion region, W, can be expressed as $W = W_p + W_i - W_d$, where W_p *is* the thickness of the $Al_{0.8}InAsSb$ p-type layer, W_i is the thickness of the unintentionally-doped multiplication layer, and W_d is the depletion region thickness, respectively.

The total current density can be obtained by substituting eqs. (2) and (3) into eq. (1). The external quantum efficiency can then be calculated using the following equation:

$$\eta_{QE} = (1-R)(1-0.22)[\left(1 - \frac{\alpha^2 L_n^2}{1-\alpha^2 L_n^2}\right) exp(-\alpha W) + \frac{\alpha L_n}{1-\alpha^2 L_n^2} exp\left(-\frac{W}{L_n}\right) - exp(-\alpha W_p - \alpha W_i)], \quad (4)$$

where R is the reflection coefficient of the top surface, about 30%; and 0.22 is the percentage of 850 nm laser absorbed in the top GaSb layer [14]. Figure 5 shows the measured external quantum efficiency of a 200 μm-diameter $Al_{0.8}InAsSb$ APD versus reverse bias from -1 V to -26 V in 1 V steps. Using eq.

This article has been accepted for publication in a future issue of this journal, but has not been fully edited. Content may change prior to final publication. Citation information: DOI 10.1109/LPT.2018.2826999, IEEE Photonics Technology Letters

(4) the efficiency at a specific wavelength can be fit with two parameters, α and L_n.

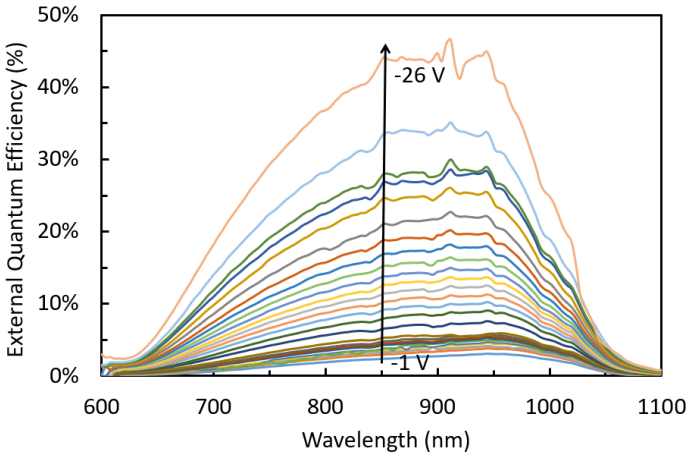

Figure 5. External quantum efficiency of a 200 μm-diameter $Al_{0.8}InAsSb$ p-i-n APD.

Figure 6 compares the measured and calculated external quantum efficiency at 850 nm for $\alpha = 5.4 \times 10^4\ cm^{-1}$, $L_n = 170\ nm$. Using two-parameter curve fitting, good agreement is achieved between the experimental and calculated quantum efficiency up to -24.5 V, which is marked by the dash line. At higher voltage, impact ionization causes the curves to diverge. Therefore, we have used -24.5 V as the unity gain point. After this bias volatge, the multiplication gain dominates the increment of the photocurrent, the change caused by extended depletion region can be ingored. And at that unity gain point the external quantum efficiency is approximately 30% at 850 nm wavelength. The external quantum efficiency is consistent with the photon responsivity from Figure 2, which is about 0.2 A/W.

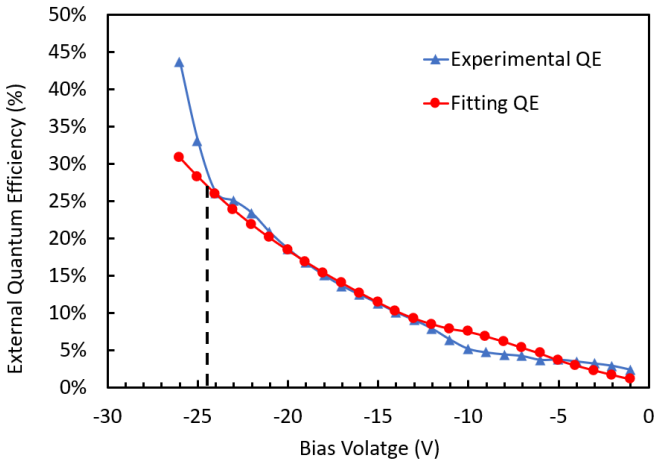

Figure 6. Two-parameter fit of the external quantum efficiency of a 200 μm-diameter $Al_{0.8}InAsSb$ p-i-n APD at 850 nm wavelength.

The unity gain point can be confirmed and the k value can be determined using a modification of the noise technique described in [15]. The shot noise power is given by [3]:

$$S = 2qI_u M^2 F(M) R(\omega), \qquad (5)$$

where I_u is the unity-gain photocurrent, $F(M)$ is the excess noise factor, and $R(\omega)$ is the frequency dependent impedance. From eq. (5), the noise power at any relative gain M_n can be expressed as:

$$S_n = 2qI_u\left(M_n M_{pt}\right)^2 F\left(M_n M_{pt}\right) R(\omega) \qquad (6)$$

where M_{pt} corresponds to the gain at the nominal unity-gain point voltage and M_n is the measured gain relative to M_{pt}. We note that M_{pt} may not be exactly unity and its actual value is determined by this procedure. The noise is measured for a series of M_n values and the follow ratio is computed

$$\frac{S_n}{S_{pt}} = M_n^2 \frac{F(M_n M_{pt})}{F\left(M_{pt}\right)}. \qquad (7)$$

The values of S_n and S_{pt} are measured, and the excess noise factors are calculated using the local field model: $F < M >= kM + (1-k)(2-1/M)$. For these measurements based on the discussion above, -24.5 was selected as the M_{pt} reference point. Figure 7 shows the experimental values of S_n/S_{pt} and a fit using M_{pt} and k as adjustable parameters. The best fit was obtained for M_{pt} =1.0, which confirms that -24.5 V is the unity gain point, and $k = 0.05$.

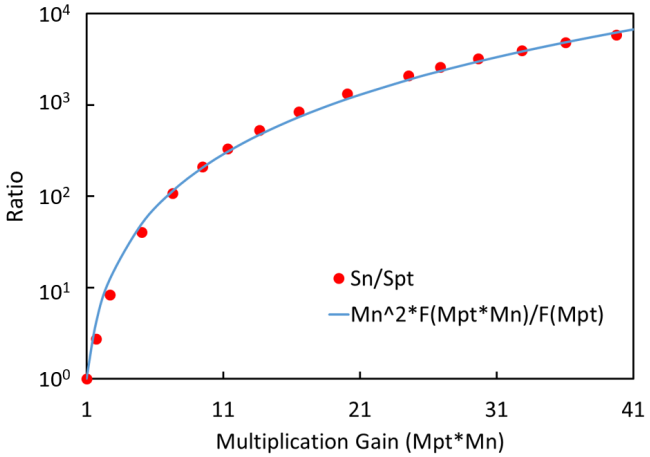

Figure 7. Two-parameters fitting curve of the gain versus ratio of excess noise.

Using -24.5 V as the unity-gain reference, the excess noise was measured with an HP 8970 noise figure meter and a 543-nm He-Ne CW laser [16], [17]. The k value was obtained using the local-field model [3] to plot and the gain values obtained as described above. The data points in Fig. 8 show the excess noise factor versus gain. The value of k is between 0.05 and 0.07 [18], which is consistent with the fitting k value from the Fig. 7.

This article has been accepted for publication in a future issue of this journal, but has not been fully edited. Content may change prior to final publication. Citation information: DOI 10.1109/LPT.2018.2826999, IEEE Photonics Technology Letters

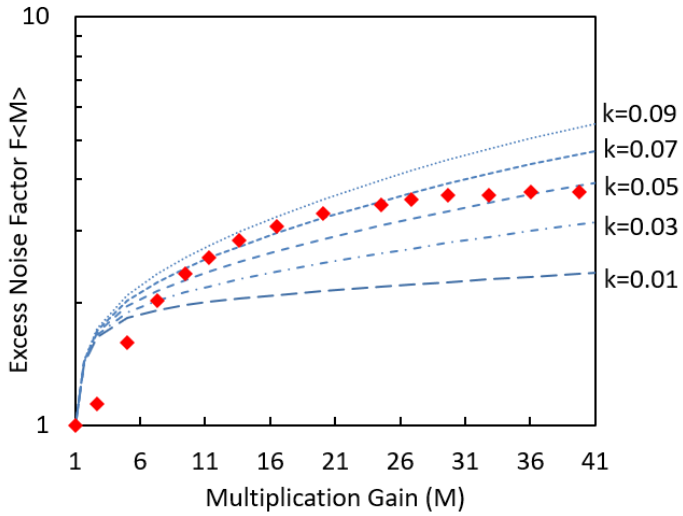

Figure 8. Excess noise factor versus gain of 100 μm-diameter $Al_{0.8}InAsSb$ p-i-n APD.

IV. Conclusion

We report $Al_{0.8}InAsSb$ p-i-n structure APDs, fabricated using the digital alloy growth technique. These APDs exhibit gain as high as 489, low excess noise corresponding to k = 0.05~0.07, and external quantum efficiency of 30% at 850 nm wavelength.

References

[1] J. C. Campbell, "Recent Advances in Avalanche Photodiodes," in *IEEE Journal of Lightwave Technology,* 34(2), 278-285 (2016).

[2] J. C. Campbell, "Advances in photodetectors," in *Optical Fiber Telecommunications, Part A: Components and Subsystems*, *5th ed.,* edited by I. Kaminow, T. Li, and A. E. Wilner (Academic Press, 2008), Vol. 5.

[3] R. J. McIntyre, "Multiplication noise in uniform avalanche photodiodes" *IEEE Trans. Electron Dev*. ED-13, 64 (1966).

[4] R. B. Emmons, *Journal of Applied Physics.* 38, 3705 (1967).

[5] X. Zhou, L. L. G. Pinel, S. J. Dimler, S. Zhang, J. S. Ng and C. H. Tan, " Thin Al1−xGaxAs0.56Sb0.44 Diodes With Low Excess Noise," in *IEEE Journal of Selected Topics in Quantum Electronics,* vol. 24, no. 2, pp. 1-5, March-April, (2018).

[6] Shiyu Xie, Xinxin Zhou, Shiyong Zhang, David J. Thomson, Xia Chen, Graham T. Reed, Jo Shien Ng, and Chee Hing Tan, "InGaAs/AlGaAsSb avalanche photodiode with high gain-bandwidth product," in *Optics Express*, 24, 24242-24247 (2016)

[7] Scott J. Maddox, Stephen D. March, and Seth R. Bank, "Broadly Tunable AlInAsSb Digital Alloys Grown on GaSb," *Crystal Growth and Design*, 16(7), 3582-3586 (2016).

[8] L. G. Vaughn, L. R. Dawson, E. A. Pease, L. F. Lester, H. Xu, Y. Jiang, and A. L. Gray, *Proc. SPIE* 5722, 307–318 (2005).

[9] L. G. Vaughn, L. Dawson, Ralph, H. Xu, Y. Jiang, and L. F. Lester, in "Characterization of AlInAsSb and AlGaInAsSb MBE-grown digital alloys", *Mat. Res. Soc. Symp. Proc.,* Vol. 744, pp. M7.2.1–M7.2.12 (2003),

[10] T. C. Shen, G. B. Gao and H. Morkoç, "Recent developments in ohmic contacts for III–V compound semiconductors," *J. Vac. Sci. Technol. B*, vol 10, pp. 2113 (1992).

[11] A.G. Baca, F. Ren, J.C. Zolper, R.D. Briggs, and S.J. Pearton, "A survey of ohmic contacts to III-V compound semiconductors," *Thin Solid Films*, pp. 308–309, pp. 599–606 (1997).

[12] Jiyuan Zheng, Lai Wang, Xingzhao Wu, Zhibiao Hao, Changzheng Sun, Bing Xiong, Yi Luo et al. "A PMT-like high gain avalanche photodiode based on GaN/AlN periodically stacked structure." *Applied Physics Letters* 109, no. 24 (2016): 241105.

[13] S.M. Sze, Kwok K. Ng, *Physics of Semiconductor Devices* (2007)

[14] Diego Martín, and Carlos Algora. "Temperature-dependent GaSb material parameters for reliable thermophotovoltaic cell modelling." in *Semiconductor Science and Technology* 19, no. 8 (2004): 1040.

[15] Han-Din Liu, Huapu Pan, Chong Hu, Dion McIntosh, Zhiwen Lu, Joe Campbell, Yimin Kang, and Mike Morse. "Avalanche photodiode punch-through gain determination through excess noise analysis." in *Journal of Applied Physics*, 106, no. 6 (2009): 064507.

[16] M. Ren, S. J. Maddox, M. E. Woodson, Y. Chen, S. R. Bank and J. C. Campbell, "Low excess noise AlxIn1-xAsySb1-y (x: 0.3~0.7) avalanche photodiodes," *2016 Conference on Lasers and Electro-Optics (CLEO)*, San Jose, CA, 2016, pp. 1-2.

[17] Madison E. Woodson, Min Ren, Scott J. Maddox, Yaojia Chen, Seth R. Bank, and Joe C. Campbell. "Low-noise AlInAsSb avalanche photodiode." in *Applied Physics Letters* 108, no. 8 (2016): 081102.

[18] J. C. Campbell, S. Chandraskhar, W. T. Tsang, G. J. Qua, and B. C. Johnson, "Multiplication noise of wide-bandwidth InP/InGaAsP/InGaAs avalanche photodiodes. " in *IEEE Journal of Lightwave Technology*, 7(3), 473 (1989).